Gamma random field simulation by a covariance matrix transformation method

Stochastic Environmental Research and Risk Assessment

ISSN 1436-3240
Volume 25
Number 2

Stoch Environ Res Risk Assess
(2010) 25:235-251
DOI 10.1007/
s00477-010-0434-8

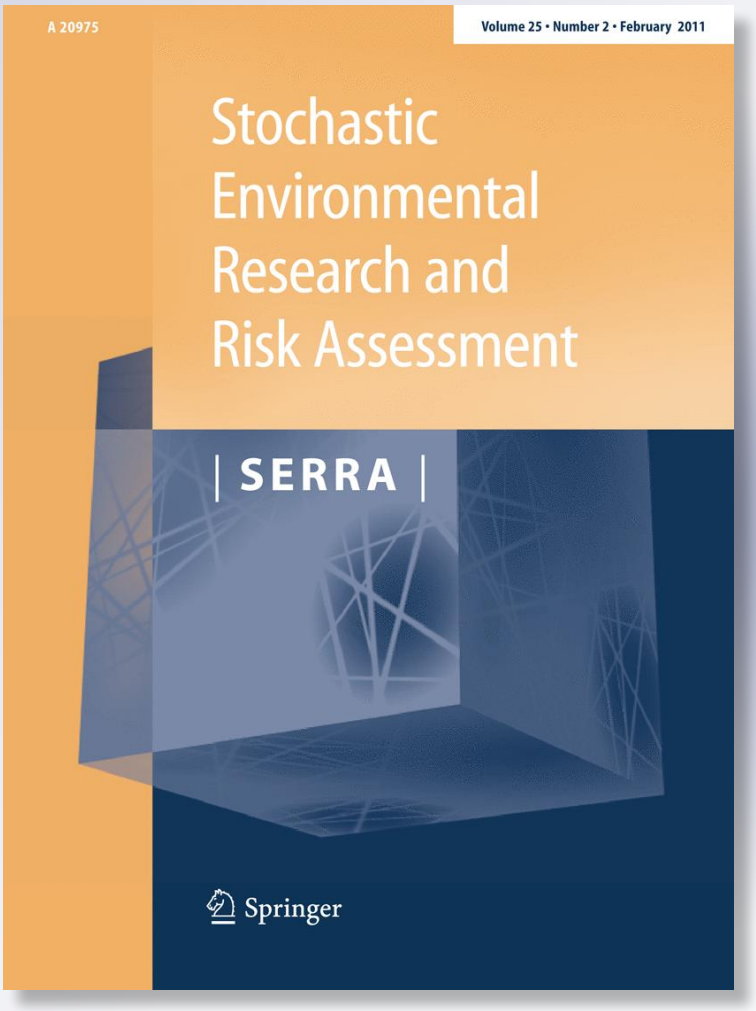

Springer

Stoch Environ Res Risk Assess (2011) 25:235–251
DOI 10.1007/s00477-010-0434-8

ORIGINAL PAPER

Gamma random field simulation by a covariance matrix transformation method

Jun-Jih Liou · Yuan-Fong Su · Jie-Lun Chiang · Ke-Sheng Cheng

Published online: 20 August 2010

Abstract In studies involving environmental risk assessment, Gaussian random field generators are often used to yield realizations of a Gaussian random field, and then realizations of the non-Gaussian target random field are obtained by an inverse-normal transformation. Such simulation process requires a set of observed data for estimation of the empirical cumulative distribution function (ECDF) and covariance function of the random field under investigation. However, if realizations of a non-Gaussian random field with specific probability density and covariance function are needed, such observed-data-based simulation process will not work when no observed data are available. In this paper we present details of a gamma random field simulation approach which does not require a set of observed data. A key element of the approach lies on the theoretical relationship between the covariance functions of a gamma random field and its corresponding standard normal random field. Through a set of devised simulation scenarios, the proposed technique is shown to be capable of generating realizations of the given gamma random fields.

J.-J. Liou · Y.-F. Su · K.-S. Cheng (✉)
Department of Bioenvironmental Systems Engineering, National Taiwan University, Taipei, Taiwan, ROC
e-mail: rslab@ntu.edu.tw

J.-L. Chiang
Department of Soil and Water Conservation, National Pingtung University of Science and Technology, Pingtung, Taiwan, ROC

K.-S. Cheng
Hydrotech Research Institute, National Taiwan University, Taipei, Taiwan, ROC

Keywords Stochastic simulation · Gamma distribution · Geostatistics · Sequential Gaussian simulation · Random field simulation

1 Introduction

Random field simulation has been widely applied to studies involving environmental risk assessment such as soil contamination (Franco et al. 2006), spatial rainfall modeling (Guillot 1999), solutes transport in a porous medium (Herrick et al. 2002), etc. Many of such applications use random field generators to generate large sets of realizations which can be characterized by the desired Gaussian distribution and spatial variation structure (or semi-variogram). The turning bands algorithm (Journel 1974), sequential Gaussian simulation (SGS) algorithm (Deutsch and Journel 1992; Goovaerts 1997) and Hydro_Gen model (Bellin and Rubin 1996) are examples of such Gaussian random field generators.

However, many hydrological and environmental variables are non-Gaussian and asymmetric. For examples, hydraulic conductivity is often considered to be log-normally distributed (Vogler and Chrysikopoulos 2001; Minasny et al. 2004) and the distribution of point rainfall is popularly modeled by gamma or log-normal distributions (Zeng et al. 2000). For practical applications involving uncertainty or risk mapping of these variables, observed data are transformed to normal scores in the beginning, and SGS is then performed in normal space. Finally, data generated by SGS are back-transformed to realizations of the target variables. In such practices, normal transformation of the observed data and inverse-normal transformation of the simulated data are generally based on the empirical cumulative distribution function (ECDF) of the

observed data. Thus, in the SGS process, the covariance function (or the semi-variogram) of the Gaussian random field is estimated using the normal scores transformed from the observed data. Theoretical relationship between the covariance functions of the observed non-Gaussian data and Gaussian-transformed scores are unknown and not explicitly dealt with in the SGS process. In general, results of SGS are evaluated by comparing empirical covariance functions of simulated realizations to empirical covariance function of the observed data. Such comparisons may encounter a high degree of uncertainty if observed data are available only at limited number of locations.

From a theoretical point of view, if we want to generate realizations of a non-Gaussian random field with specific probability density and covariance function when observed data are not available, the above *observed-data-based* SGS process will not work since the covariance function of the Gaussian random field cannot be estimated without a set of normal scores transformed from the observed data. Specifically, covariance functions of the non-Gaussian random field and its corresponding Gaussian random field are not the same. Thus, a key element of the Gaussian-transform approach lies on determining the spatial variation structure (i.e. the covariance function) of the Gaussian random field, given the spatial variation structure of the non-Gaussian random field.

Cheng et al. (2010) proposed a frequency-factor-based bivariate gamma simulation approach. The approach basically generates a random sample $\{\{(u_i, v_i),\ i = 1, \ldots, n\}$ of the bivariate standard normal variates (U, V) whose correlation coefficient (ρ_{UV}) is consistent with the correlation coefficient (ρ_{XY}) of the desired bivariate gamma random variates (X, Y). Then a set of random sample of (X, Y), say $\{(x_i, y_i),\ i = 1, \ldots, n\}$ is obtained by employing a transformation of $\{(u_i, v_i),\ i = 1, \ldots, n\}$ which involves the frequency factor equation and the general equation for hydrological frequency analysis. A key element of the approach lies on a one-to-one conversion between ρ_{UV} and ρ_{XY} which ensures the random sample $\{(x_i, y_i)\ i = 1, \ldots, n\}$ having the desired statistical properties of (X, Y) including the means, standard deviations and the correlation coefficient. Extending from the bivariate case, stochastic simulation of a gamma random field can be achieved in a similar manner. Many geophysical and hydrological variables such as the topographical index (Niu et al. 2005), base flow (Botter et al. 2007), and soil moisture content (Rodriguez-Iturbe et al. 1999; Potter et al. 2005) are non-negative and asymmetrically distributed, and may be treated as gamma random variables. Additionally, a few studies have found that spatial variation of the natural processes and environmental and health risks can be well characterized by gamma random fields. Rauch (1997) studied the surface displacements due to liquefaction-induced lateral deformation in earthquakes and found the variation in horizontal displacement across the surface area could be effectively characterized by the gamma distribution. Wolpert and Ickstadt (1998) proposed a Poisson/gamma random field model to analyze the density and spatial correlation of hickory trees in a research plot. Best et al. (2000) used a hierarchical Poisson/gamma random field model to study the risk of respiratory disorders in children due to traffic pollution. Høst et al. (2002) used acoustic echo data from a transect survey to map the abundance of Norwegian spring-spawning herring. They modeled the acoustic echo data as a gamma random field and accounted for possible space–time autocorrelations. Nieto-Barajas (2008) introduced a Markov gamma random field for modeling relative risks in disease mapping data. In a case study in polluted soil management, Emery (2008) used a gamma random field model to quantify the risk that heavy metal (lead) concentrations over remediation units exceed a regulatory toxicity level. It was found that the proposed gamma random field model could account for an asymmetry in the spatial correlation of the indicator functions around the median and for a spatial clustering of high pollutant concentrations. Therefore, development of a gamma random field simulation approach is peremptory for the purpose of uncertainty assessment of these natural and environmental processes.

In this paper we present details of a gamma random field simulation approach. Section 2 briefly describes characteristics of a random field. Section 3 gives a conceptual description of the proposed gamma random field simulation approach. Section 4 forms the theoretical developments of the proposed approach including a sequential Gaussian simulation algorithm based on conditional multivariate normal density, conversion of covariance matrices between the gamma and standard Gaussian random fields, and transforming Gaussian realizations to gamma realizations. In Sect. 5, a set of simulation scenarios are devised for validation of the proposed approach. A few concluding remarks are given in Sect. 6.

2 Characterizing a random field

A random variable is completely characterized by its probability density function (PDF) or cumulative distribution function (CDF). A pair of jointly distributed bivariate random variables can be completely characterized by the marginal densities and their correlation coefficient. Similarly, characterizing a random field $\{Z(x),\ x \in \Omega\}$ over a spatial domain Ω requires knowing the probability density function $f_Z(x)$ for every $x \in \Omega$ and the covariance function $\mathrm{Cov}(Z(x), Z(x')) = C(x, x')$ (or correlation) of any pair of random variables $[Z(x),\ Z(x');\ x,\ x' \in \Omega]$. If the random

field $\{Z(x),\ x \in \Omega\}$ is stationary, the probability density function $f_Z(x)$ is independent of the location x and the covariance function $C(x, x')$ depends only on the distance between x and x', i.e.,

$$C(x, x') = C(|x - x'|) \quad \text{for all } x, x' \in \Omega \tag{1}$$

In geostatistics, spatial variation of a random field is often expressed in terms of the semi-variogram $\gamma(x, x')$ defined as

$$\gamma(x, x') = \frac{1}{2} E\left[(Z(x) - Z(x'))^2\right], \quad x, x' \in \Omega. \tag{2}$$

For a stationary random field, the semi-variogram is also independent of the locations x and x', and the following relationship between the covariance function and the semi-variogram exists

$$\gamma(h) = C(0) - C(h) \tag{3}$$

where $h = |x - x'|$ represents the distance between x and x' and $C(0)$ is the variance of the random variable $Z(x)$, i.e. σ_Z^2. A semi-variogram increases with the separation distance between x and x', and a typical form of the semi-variogram is shown in Fig. 1a.

A semi-variogram is characterized by its *sill* and *range*. The sill represents the asymptotic value of the semi-variogram and is numerically equal to σ_Z^2. The range is the minimum distance $h = |x - x'|$ beyond which two random variables $Z(x)$ and $Z(x')$ become independent. If the range equals zero, the random field lacks spatial correlation and is associated with a semi-variogram with the pure nugget effect (see Fig. 1b). A semi-variogram must possess certain statistical properties and not arbitrary functions can be a valid semi-variogram. Thus, feasible variogram models have been developed to characterize the spatial variation of random fields. Readers are referred to Journel and Huijbregts (1978) and Cheng et al. (2003) for more details about properties and modeling of the semi-variogram. Table 1 presents some of the commonly used semi-variogram models.

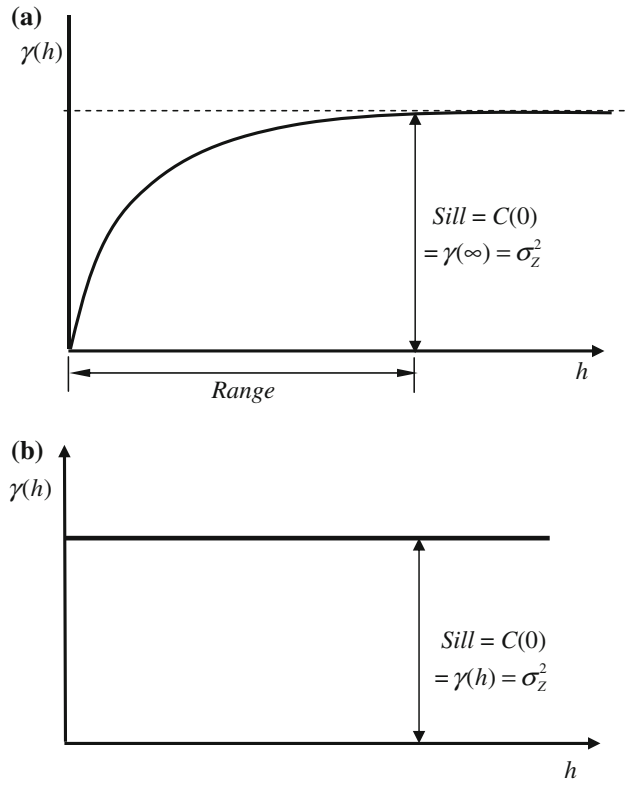

Fig. 1 A typical semi-variogram (**a**) and a pure-nugget semi-variogram (**b**)

Table 1 Commonly used semi-variogram models

Model type	Function of $\gamma(h)$	Range	Sill
Exponential	$\gamma(h) = \omega[1 - \exp(-h/a)]$	$3a$	ω
Spherical	$\gamma(h) = \begin{cases} \omega\left[\frac{3}{2}(h/a) - \frac{1}{2}(h/a)^3\right], & h \le a \\ \omega, & h > a \end{cases}$	a	ω
Gaussian	$\gamma(h) = \omega[1 - \exp[-(h/a)^2]]$	$\sqrt{3}a$	ω
Power	$\gamma(h) = \omega h^{\alpha}$, $\alpha < 2$	$+\infty$	N/A

3 Conceptual description of a gamma random field simulation approach

Based on the bivariate gamma simulation approach proposed by Cheng et al. (2010), simulation of a gamma random field can be achieved in a similar, yet more complicated, manner. Through a theoretical conversion between ρ_{UV} and ρ_{XY}, random samples of a pair of bivariate gamma random variates (X, Y) with desired marginal densities [which are fully characterized by the means (μ_X, μ_Y) and coefficients of skewness (γ_X, γ_Y)] and correlation coefficient ρ_{XY} can be obtained by firstly generating random samples of a corresponding pair of bivariate variates (U, V) with standard normal density and correlation coefficient ρ_{UV}, and a subsequent Gaussian-to-gamma transformation. In contrast to stochastic simulation of bivariate random variables which involves correlation between only one pair of random variables, stochastic simulation of a random field $Z(x)$ involves correlations among a set of random variables which are expressed in terms of a multivariate covariance (or correlation) matrix. Figure 2 illustrates the conceptual process for stochastic simulation of bivariate gamma distribution and gamma random field. For random field simulation, the whole process is composed of three sequential components:

Converting the covariance function $C_Z(h)$ of a gamma random field $Z(x)$ to the covariance function $C_W(h)$ of a corresponding Gaussian random field $W(x)$. In a sequential random field simulation process, the covariance function

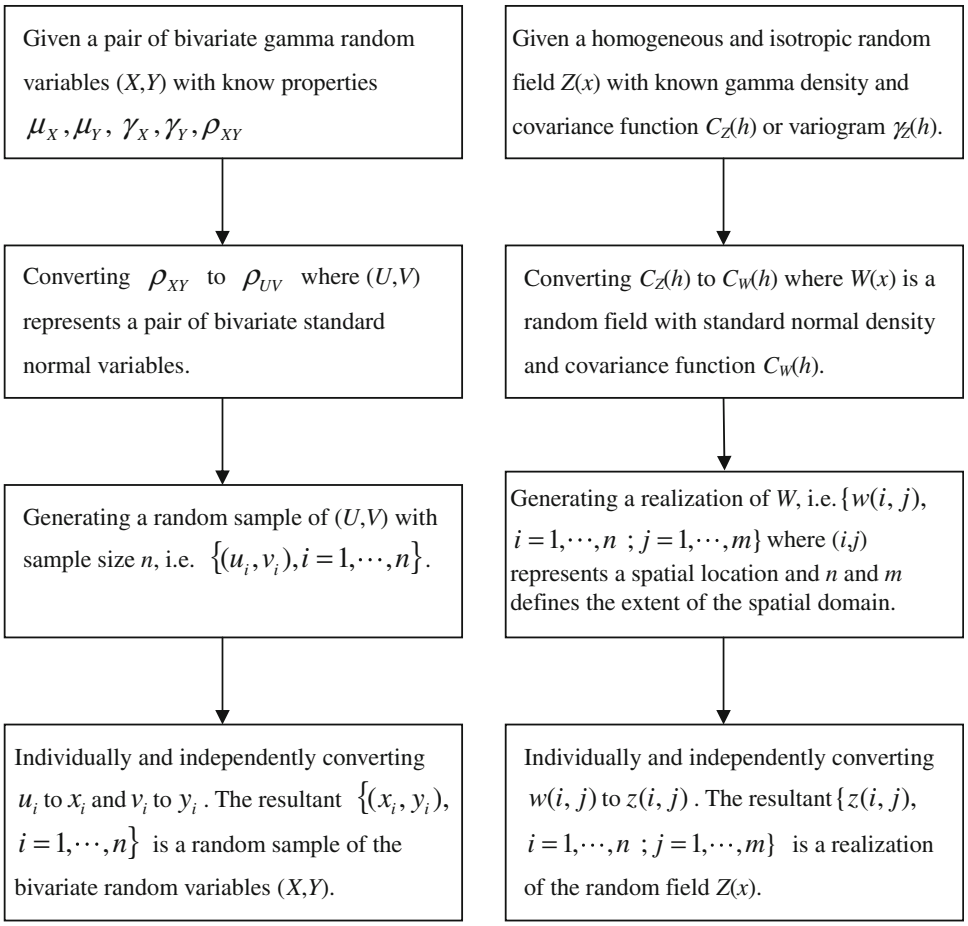

Fig. 2 Conceptual flowcharts for stochastic simulation of a bivariate gamma distribution (*left*) and a gamma random field (*right*)

appears as a covariance matrix Σ which involves a target point for random number generation and its neighboring points. Thus, conversion between the covariance function $C_Z(h)$ and $C_W(h)$ is equivalent to conversion between the covariance matrices Σ_Z and Σ_W.

(1) Generating realizations of the Gaussian random field with covariance function $C_W(h)$, and
(2) Transforming realizations of $W(x)$ to corresponding realizations of the gamma random field $Z(x)$.

In the following sections we present detailed procedures of the three components. For convenience of explanation, we begin with an introduction of the sequential Gaussian simulation, although the simulation process starts with the conversion of covariance matrices, as illustrated in Fig. 2.

4 Methodology and detailed procedures

4.1 Sequential Gaussian simulation

Given a homogeneous and isotropic random field $\{Z(x), x \in \Omega\}$ with known probability density function $f_Z(z)$ and covariance function $C_Z(h)$ (or semi-variogram $\gamma_Z(h)$), we want to generate as many random samples (realizations) of the random field.

For a set of $(p + q)$ normally distributed random variables, say $W' = (W_1, \ldots, W_{p+q})$, the multivariate joint density is given by Morrison (1990)

$$f_W(w) = \frac{1}{(2\pi)^{(p+q)/2}|\Sigma_W|^{1/2}} e^{-\frac{1}{2}(w-\mu)'\Sigma_W^{-1}(w-\mu)}, \tag{4}$$

where Σ_W is the covariance matrix with $(p + q) \times (p + q)$ dimension and μ is the $(p + q)$ dimensional mean vector. Let W be divided into two subsets $W_1' = (W_1, \ldots, W_p)$, and $W_2' = (W_{p+1}, \ldots, W_{p+q})$, the mean vector and the covariance matrix can thus be respectively expressed as

$$\mu = \begin{bmatrix} \mu_1 \\ \mu_2 \end{bmatrix} \tag{5}$$

and

$$\Sigma_W = \begin{bmatrix} \Sigma_{11} & \Sigma_{12} \\ \Sigma_{12}' & \Sigma_{22} \end{bmatrix}, \tag{6}$$

where μ_1 and μ_2 are respectively the mean vectors of W_1 and W_2, and Σ_{ij} is the covariance matrix of W_i and W_j $(i, j = 1$ or $2)$.

Suppose that values of W_2 are known, i.e. $w_2' = (w_{p+1}, \ldots, w_{p+q})$, the conditional multivariate density of W_1 given $W_2 = w_2$ can then be expressed by Morrison (1990)

$$f_{W_1|W_2}(w_1|w_2) = \frac{1}{(2\pi)^{p/2}|\Sigma^*|^{1/2}} e^{-\frac{1}{2}(w_1-\mu^*)'(\Sigma^*)^{-1}(w_1-\mu^*)} \quad (7)$$

where

$$\mu^* = \mu_{W_1|w_2} = \mu_1 + \Sigma_{12}\Sigma_{22}^{-1}(w_2 - \mu_2) \quad (8)$$

$$\Sigma^* = \Sigma_{W_1|w_2} = \Sigma_{11} - \Sigma_{12}\Sigma_{22}^{-1}\Sigma_{12}' \quad (9)$$

Equation 7 lays the foundation for stochastic simulation of a Gaussian random field. Random field simulation is generally carried out by sequentially generating random number at only one target location each time. Thus, for sequential stochastic simulation of a standard Gaussian random field, μ_1 and Σ_{11}, respectively reduce to 0 and 1, and the covariance matrix in Eq. 6 becomes

$$\Sigma_W = \begin{bmatrix} C_{11} & C_{12} & \cdots & C_{1,1+q} \\ C_{21} & C_{22} & \cdots & C_{2,1+q} \\ \vdots & \vdots & \ddots & \vdots \\ C_{1+q,1} & C_{1+q,2} & \cdots & C_{1+q,1+q} \end{bmatrix} = \begin{bmatrix} \Sigma_{11} & \Sigma_{12} \\ \Sigma_{12}' & \Sigma_{22} \end{bmatrix} \quad (10)$$

where C_{ij} represents the covariance between two univariate random variables W_i and W_j, and $C_{ii} = 1$ for all $i = 1,\ldots,1+q$. Notice the apparent correspondence of $[C_{ij}]$ and Σ_{kl} by matrix partition in the above equation.

Suppose that the random field simulation begins with a univariate random number generation at an initial point x_o of coordinate (1,1) (see Fig. 3a). We then sequentially generate random numbers at other locations under the condition of previously generated random numbers. Such conditional simulation can be done by using Eqs. 7, 8 and 9. The simulation is conducted following a column-preference style in which random numbers at all nodes of the same line are generated sequentially and then the process proceeds to the next line (see Fig. 3b). At any stage of the simulation process, the number and locations of the conditioning variates depend on the range measured in terms of the grid interval. For example, the range is shown to be twice of the grid interval in Fig. 3c and Fig. 3d demonstrates that only six neighboring points are included in the conditional simulation of $W(i, j)$. Generated random numbers of these conditioning variates form the condition vector w_2 in Eqs. 7 and 8. Finally, the covariance matrices Σ_{kl} ($k, l = 1$ or 2) and Σ^* can be established using the given semi-variogram $\gamma(h)$ or covariance function $C(h)$ of the random field. In our random field simulation approach, the covariance matrix Σ_W is obtained by transforming from the covariance matrix of a corresponding gamma random field to ensure the resultant realizations of the gamma random field having desired statistical properties. Details of such transformation are given in the following subsection.

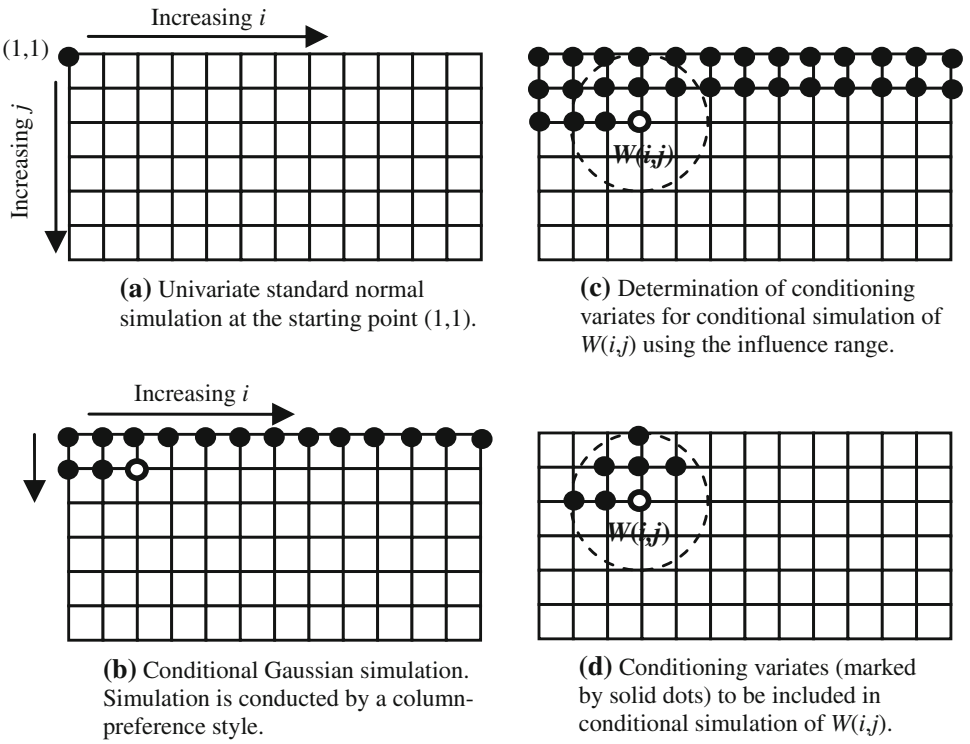

(a) Univariate standard normal simulation at the starting point (1,1).

(c) Determination of conditioning variates for conditional simulation of $W(i,j)$ using the influence range.

(b) Conditional Gaussian simulation. Simulation is conducted by a column-preference style.

(d) Conditioning variates (marked by solid dots) to be included in conditional simulation of $W(i,j)$.

Fig. 3 Illustration of a sequential column-preference generation algorithm. *Solid dots* represent nodes at which random numbers have been generated and the *empty dot* is the target node where random number is to be generated conditioning on the generated numbers within a *circle* of radius a (range of the random field)

4.2 Covariance matrices conversion

Section 4.1 gives details for stochastic simulation of a standard Gaussian random field $W(x)$ with covariance function $C_W(h)$ or variogram $\gamma_W(h)$. However, our objective is to generate realizations of a gamma random field $Z(x)$ with a desired probability density function $f_Z(z)$ and a given covariance function $C_Z(h)$ or variogram $\gamma_Z(h)$. A gamma-field counter part of Σ_W can be expressed by

$$\Sigma_Z = \begin{bmatrix} \Sigma_{11}^G & \Sigma_{12}^G \\ \Sigma_{12}^{G'} & \Sigma_{22}^G \end{bmatrix} \tag{11}$$

In the previous section we have implicitly assumed that the covariance function $C_W(h)$ is given or known. Such assumption raises a question of how can we be sure that our stochastic simulation process using the assumed $C_W(h)$ will eventually yield realizations of $Z(x)$ which are associated with the desired covariance function $C_Z(h)$. Apparently, the covariance function $C_W(h)$ cannot be arbitrarily chosen and a conversion between $C_W(h)$ and $C_Z(h)$ (or between Σ_Z and Σ_W) is necessitated.

Similar to the conversional relationship between correlation coefficients of the bivariate gamma and bivariate normal densities derived by Cheng et al. (2010), we present in this section another form of the conversional relationship.

Let X be a gamma random variable, i.e., $X \sim G(\alpha, \lambda)$, with the following density

$$f_X(x) = \frac{\lambda^\alpha}{\Gamma(\alpha)} x^{\alpha-1} e^{-\lambda x}, \alpha, \lambda > 0 \quad \text{and} \quad 0 \le x < +\infty. \tag{12a}$$

$$\mu_X = \alpha/\lambda, \tag{12b}$$

$$\sigma_X = \sqrt{\alpha}/\lambda, \tag{12c}$$

$$\gamma_X = 2/\sqrt{\alpha} \tag{12d}$$

where μ_X, σ_X and γ_X are respectively the mean, standard deviation and coefficient of skewness of X. We define a new random variable $Y = g(X) = 2\lambda X$ and the PDF of Y can be derived by transformation of random variables.

$$f_Y(y) = f_X(g^{-1}(y)) \left| \frac{dg^{-1}(y)}{dy} \right| \tag{13}$$

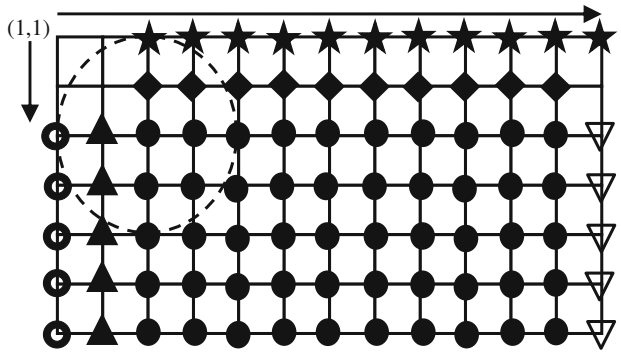

Fig. 4 Illustration of nodes with common covariance matrix for conditional simulation using a column-preference generation algorithm. *Nodes* marked by the same *symbols* have a common covariance matrix Σ_W. (The range is assumed to be twice of the grid interval.)

$$f_Y(y) = \frac{\lambda^\alpha}{\Gamma(\alpha)} \left(\frac{y}{2\lambda}\right)^{\alpha-1} e^{-\lambda y/(2\lambda)} \frac{1}{2\lambda} = \frac{1}{\Gamma(\alpha) 2^\alpha} y^{\alpha-1} e^{-y/2} \tag{14}$$

Equation 14 represents a χ^2 density with degree of freedom $k = 2\alpha$, i.e. $Y \sim \chi^2(k)$. An approximation of the χ^2 distribution by the standard normal distribution, known as the Wilson–Hilferty approximation, is given as follows (Patel and Read 1996)

$$y \approx 2\alpha \left\{ 1 - \frac{1}{9\alpha} + w\sqrt{\frac{1}{9\alpha}} \right\}^3 \tag{15}$$

where w represents the standard normal deviate and y is the corresponding χ^2 variate. Substituting the relationship $Y = 2\lambda X$ into Eq. 15 yields the transformation between the standard normal deviate w and gamma variate x, i.e.,

$$x = \frac{y}{2\lambda} \approx \frac{\alpha}{\lambda} \left\{ 1 - \frac{1}{9\alpha} + w\sqrt{\frac{1}{9\alpha}} \right\}^3. \tag{16}$$

Equation 16 is a one-to-one mapping function between x and w (see the proof given in Appendix 1) and the expected value of X equals $\frac{\alpha}{\lambda}$. Thus, given a large set of standard normal random numbers, say $\{w_i, i = 1, 2,\ldots,n\}$, the sample average of $\left\{1 - \frac{1}{9\alpha} + w_i\sqrt{\frac{1}{9\alpha}}\right\}^3, i = 1, 2, \ldots, n$, should be very close to unity to ensure high approximation accuracy by the Wilson–Hilferty approximation. A simple check (demonstrated in Table 2) of the approximation

Table 2 Accuracy check for the Wilson–Hilferty approximation

α	0.15	0.2	0.3	0.4	0.5	1.0	1.5	2.0	3.0
γ	5.164	4.472	3.651	3.162	2.828	2	1.633	1.414	1.155
T (n = 1,000)	0.579	0.822	0.950	0.983	0.995	1.006	1.006	1.006	1.005
T (n = 10,000)	0.584	0.815	0.937	0.968	0.980	0.995	0.997	0.998	0.999

$T = \frac{1}{n}\sum_{i=1}^{n}\left(1 - \frac{1}{9\alpha} + w_i\sqrt{\frac{1}{9\alpha}}\right)^3 \cdot \gamma = \frac{2}{\sqrt{\alpha}}$ is the coefficient of skewness of the gamma random variable X in Eq. 16

Table 3 Parameters of the gamma density and spherical semi-variogram model designated for random field stochastic simulation

Scenario type	Gamma density parameters				Variogram parameters		Size of simulation[a]
	μ	γ	α	λ	$\omega = \sigma^2$	a	
I	0.67	2.985	0.449	0.67	1	1, 2, 3, 6	80 × 80
							40 × 40
II	1	2	1	1	1	1, 2, 3, 6	80 × 80
							40 × 40
III	2	1	4	2	1	1, 2, 3, 6	80 × 80
							40 × 40
IV	4	0.5	16	4	1	1, 2, 3, 6	80 × 80
							40 × 40

[a] Size of simulation represents the spatial domain Ω of the random field $Z(x)$. For a simulation run with 80 × 80 size of simulation, the random field is represented by $Z(x)$, $x \in \Omega = \{(i,j),\ i = 1,2,\ldots,80;\ j = 1,2,\ldots,80\}$

Table 4 Summary statistics of the parameter estimators of the density function and the semi-variogram model ($\hat{\mu}_Z, \hat{\sigma}_Z, \hat{\gamma}_Z, \hat{\omega}, \hat{a}$)—Scenario I

Parameter estimator	Summary statistics	a (Range of the semi-variogram)			
		1	2	3	6
Size of simulation 80 × 80 ($\mu = 0.67$, $\gamma = 2.985$, $\omega = \sigma^2 = 1$)					
$\hat{\mu}_Z$	Mean	0.6611	0.6595	0.6593	0.6771
	SD	0.0138	0.0202	0.0375	0.0889
	CV	0.0208	0.0307	0.0569	0.1314
$\hat{\sigma}_Z$	Mean	0.9930	0.9738	0.9874	1.0286
	SD	0.0542	0.0758	0.1004	0.2229
	CV	0.0546	0.0779	0.1017	0.2167
$\hat{\gamma}_Z$	Mean	3.1958	3.0818	3.1665	2.9594
	SD	0.3647	0.2408	0.3156	0.3702
	CV	0.1141	0.0781	0.0997	0.1251
$\hat{\omega}$	Mean	0.9933	0.9735	0.9886	1.0496
	SD	0.0569	0.0787	0.1080	0.2421
	CV	0.0573	0.0808	0.1093	0.2307
$\hat{a}$	Mean	NA	2.1162	3.1601	6.1801
	SD	NA	0.0852	0.1425	0.4537
	CV	NA	0.0403	0.0451	0.0734
Size of simulation 40 × 40 ($\mu = 0.67$, $\gamma = 2.985$, $\omega = \sigma^2 = 1$)					
$\hat{\mu}_Z$	Mean	0.6613	0.6579	0.6564	0.6504
	SD	0.0261	0.0345	0.0739	0.1783
	CV	0.0395	0.0524	0.1126	0.2741
$\hat{\sigma}_Z$	Mean	0.9836	0.9745	0.9746	0.9257
	SD	0.1040	0.1203	0.2047	0.5135
	CV	0.1057	0.1235	0.2100	0.5547
$\hat{\gamma}_Z$	Mean	3.1327	3.1175	3.0835	2.7188
	SD	0.5499	0.4241	0.6299	0.5613
	CV	0.1755	0.1360	0.2043	0.2064
$\hat{\omega}$	Mean	0.9824	0.9781	0.9775	0.9518
	SD	0.1064	0.1262	0.2147	0.5690
	CV	0.1083	0.1290	0.2196	0.5978
$\hat{a}$	Mean	NA	2.0692	3.1096	5.7735
	SD	NA	0.1295	0.2445	0.5304
	CV	NA	0.0626	0.0786	0.0919

CV coefficient of variation

accuracy using different sets of standard normal random numbers ($n = 1{,}000$ and 10,000) reveals that the Wilson–Hilferty approximation works well for $\alpha \geq 0.5$.

The covariance of two gamma random variables X_1 and X_2 can then be related to covariance of two corresponding standard normal random variables W_1 and W_2, i.e. $\rho_{W_1W_2}$, by the following equation:

$$\begin{aligned}\mathrm{COV}(X_1,X_2) &= E\left[\left(X_1-\mu_{X_1}\right)\left(X_2-\mu_{X_2}\right)\right] \\ &= E[X_1X_2] - \left(\frac{\alpha_1\alpha_2}{\lambda_1\lambda_2}\right) \\ &\approx \left(\frac{\alpha_1\alpha_2}{\lambda_1\lambda_2}\right)\left(A + B\rho_{W_1W_2} + C\rho_{W_1W_2}^2 + D\rho_{W_1W_2}^3\right) \\ &\quad - \left(\frac{\alpha_1\alpha_2}{\lambda_1\lambda_2}\right) \end{aligned} \tag{17}$$

where $\xi_1 = \frac{1}{9\alpha_1}$, $\xi_2 = \frac{1}{9\alpha_2}$, and

$$\begin{aligned} A &= (1-\xi_1)^3(1-\xi_2)^3 + 3(1-\xi_1)\xi_1(1-\xi_2)^3 \\ &\quad + 3(1-\xi_1)^3(1-\xi_2)\xi_2 + 9(1-\xi_1)\xi_1(1-\xi_2)\xi_2 \\ B &= 9(1-\xi_1)^2\xi_1^{0.5}(1-\xi_2)^2\xi_2^{0.5} + 9\xi_1^{1.5}(1-\xi_2)^2\xi_2^{0.5} \\ &\quad + 9(1-\xi_1)^2\xi_1^{0.5}\xi_2^{1.5} + 9\xi_1^{1.5}\xi_2^{1.5} \\ C &= 18(1-\xi_1)\xi_1(1-\xi_2)\xi_2 \\ D &= 6\xi_1^{1.5}\xi_2^{1.5} \end{aligned}$$

The approximation by Eq. 17 works well for α_1, $\alpha_2 \geq 0.5$, or equivalently, coefficients of skewness of X_1 and X_2 being less than 3.0.

Derivation of the above result requires the following moments of standard normal density and moments of

Table 5 Summary statistics of the parameter estimators of the density function and the semi-variogram model ($\hat{\mu}_Z, \hat{\sigma}_Z, \hat{\gamma}_Z, \hat{\omega}, \hat{a}$)—Scenario II

Parameter estimator	Summary statistics	*a* (Range of the semi-variogram)			
		1	2	3	6
Size of simulation 80 × 80 ($\mu = 1$, $\gamma = 2$, $\omega = \sigma^2 = 1$)					
$\hat{\mu}_Z$	Mean	0.9975	0.9984	0.9981	1.0127
	SD	0.0132	0.0173	0.0319	0.0613
	CV	0.0132	0.0174	0.0320	0.0605
$\hat{\sigma}_Z$	Mean	0.9921	1.0013	0.9959	0.9931
	SD	0.0390	0.0451	0.0705	0.1229
	CV	0.0393	0.0450	0.0708	0.1237
$\hat{\gamma}_Z$	Mean	2.0540	2.0756	2.0596	1.9360
	SD	0.1155	0.1355	0.1426	0.1582
	CV	0.0563	0.0653	0.0693	0.0817
$\hat{\omega}$	Mean	0.9929	1.0005	0.9953	1.0013
	SD	0.0397	0.0465	0.0728	0.1331
	CV	0.0400	0.0465	0.0731	0.1330
$\hat{a}$	Mean	NA	2.0397	3.0066	6.1117
	SD	NA	0.0632	0.4482	0.3144
	CV	NA	0.0310	0.1491	0.0514
Size of simulation 40 × 40 ($\mu = 1$, $\gamma = 2$, $\omega = \sigma^2 = 1$)					
$\hat{\mu}_Z$	Mean	0.9952	0.9956	0.9935	1.0532
	SD	0.0238	0.0384	0.0591	0.1114
	CV	0.0239	0.0386	0.0595	0.1058
$\hat{\sigma}_Z$	Mean	0.9911	0.9896	0.9753	1.0464
	SD	0.0745	0.0981	0.1243	0.2188
	CV	0.0751	0.0991	0.1274	0.2091
$\hat{\gamma}_Z$	Mean	2.0419	2.0414	1.9918	1.8533
	SD	0.2181	0.2295	0.2980	0.3118
	CV	0.1068	0.1124	0.1496	0.1682
$\hat{\omega}$	Mean	0.9919	0.9863	0.9803	1.0723
	SD	0.0756	0.1031	0.1243	0.2379
	CV	0.0763	0.1046	0.1268	0.2219
$\hat{a}$	Mean	NA	2.0047	2.9973	5.9531
	SD	NA	0.0932	0.3377	0.6142
	CV	NA	0.0465	0.1127	0.1032

CV coefficient of variation

products of two standard normal random variables (Kendall and Stuart 1977; Kan 2008; Cheng et al. 2010)

$$E(W_1W_2) = \rho_{W_1W_2} \tag{18}$$

$$E\left(W_1^2\right) = E\left(W_2^2\right) = 1 \tag{19}$$

$$E\left(W_1^2W_2^2\right) = 2\rho_{W_1W_2}^2 + 1 \tag{20}$$

$$E\left(W_1^3W_2^3\right) = 6\rho_{W_1W_2}^3 + 9\rho_{W_1W_2} \tag{21}$$

$$E\left(W_1^3W_2\right) = E\left(W_1W_2^3\right) = 3\rho_{W_1W_2} \tag{22}$$

As depicted in Fig. 3d, random number generation at a certain node only requires previously generated random numbers at a few neighboring nodes, and these pre-generated numbers form the condition vector w_2 in Eqs. 7 and 8. Thus, we first establish the gamma-field covariance matrix Σ_Z by considering the geometric layout of the target node and its neighboring nodes and the covariance function $C_Z(h)$ or variogram $\gamma_Z(h)$ of the gamma random field $Z(x)$. Then, Eq. 17 is used to convert entry values in Σ_Z to their corresponding values in Σ_W. Finally, the covariance matrix Σ_W is used for stochastic simulation of the standard Gaussian random field following procedures described in Sect. 4.1. It should be emphasized that the covariance matrices conversion is unique since the conversional relationship in Eq. 17 is also a single-value function. The proof is given in Appendix 2.

Table 6 Summary statistics of the parameter estimators of the density function and the semi-variogram model $(\hat{\mu}_Z, \hat{\sigma}_Z, \hat{\gamma}_Z, \hat{\omega}, \hat{a})$—Scenario III

Parameter estimator	Summary statistics	*a* (Range of the semi-variogram)			
		1	2	3	6
Size of simulation 80 × 80 ($\mu = 2$, $\gamma = 1$, $\omega = \sigma^2 = 1$)					
$\hat{\mu}_Z$	Mean	1.9986	2.0013	1.9989	2.0232
	SD	0.0123	0.0192	0.0283	0.0620
	CV	0.0062	0.0096	0.0142	0.0307
$\hat{\sigma}_Z$	Mean	0.9976	1.0010	1.0089	1.0338
	SD	0.0223	0.0285	0.0414	0.0930
	CV	0.0224	0.0285	0.0411	0.0899
$\hat{\gamma}_Z$	Mean	1.0038	1.0164	1.0158	0.9967
	SD	0.0511	0.0577	0.0696	0.1158
	CV	0.0509	0.0568	0.0685	0.1162
$\hat{\omega}$	Mean	0.9976	1.0014	1.0098	1.0372
	SD	0.0227	0.0295	0.0429	0.0927
	CV	0.0227	0.0294	0.0425	0.0894
$\hat{a}$	Mean	NA	2.0115	3.0631	6.0735
	SD	NA	0.0484	0.0765	0.3777
	CV	NA	0.0241	0.0250	0.0622
Size of simulation 40 × 40 ($\mu = 2$, $\gamma = 1$, $\omega = \sigma^2 = 1$)					
$\hat{\mu}_Z$	Mean	1.9947	1.9976	2.0026	2.0029
	SD	0.0239	0.0384	0.0600	0.1144
	CV	0.0120	0.0192	0.0299	0.0571
$\hat{\sigma}_Z$	Mean	0.9892	1.0056	1.0037	0.9842
	SD	0.0478	0.0622	0.0789	0.1237
	CV	0.0483	0.0619	0.0786	0.1257
$\hat{\gamma}_Z$	Mean	1.0012	1.0149	1.0080	0.9381
	SD	0.1141	0.1078	0.1276	0.1639
	CV	0.1140	0.1063	0.1266	0.1747
$\hat{\omega}$	Mean	0.9904	1.0067	1.0067	1.0107
	SD	0.0485	0.0634	0.0833	0.1402
	CV	0.0490	0.0630	0.0827	0.1387
$\hat{a}$	Mean	NA	2.0055	3.0070	6.0622
	SD	NA	0.0868	0.1589	0.7176
	CV	NA	0.0433	0.0528	0.1184

CV coefficient of variation

4.3 Transforming Gaussian realizations to gamma realizations

We have shown that random number transformation from the standard Gaussian to gamma random variable can be achieved by using Eq. 16. Since realizations of the standard Gaussian random field are generated using a covariance matrix Σ_W which is consistent with the corresponding gamma-field covariance matrix Σ_Z and both Eqs. 16 and 17 are one-to-one single value functions, point-to-point transformation using Eq. 16 will yield a unique gamma-field realization with the desired statistical properties.

We end this section with the following summary of the simulation procedures:

(1) Generate a standard Gaussian random number at the initial node (1,1).

Determine neighboring nodes to be involved in the subsequent simulation by considering range of the random field $Z(x)$, and use the covariance function $C_Z(h)$ to establish the covariance matrix Σ_Z,

Transform Σ_Z to Σ_W using Eq. 17,

(2) Generate a standard Gaussian number at the target node using the conditional Gaussian density of Eq. 7,

(3) Repeat procedures (2)–(4) until a realization of the standard Gaussian random field is established,

(4) Perform point-to-point Gaussian-to-gamma transformation using Eq. 16, and it yields a realization of the gamma random field with desired properties.

Table 7 Summary statistics of the parameter estimators of the density function and the semi-variogram model $(\hat{\mu}_Z, \hat{\sigma}_Z, \hat{\gamma}_Z, \hat{\omega}, \hat{a})$—Scenario IV

Parameter estimator	Summary statistics	a (Range of the semi-variogram)			
		1	2	3	6
Size of simulation 80 × 80 ($\mu = 4$, $\gamma = 0.5$, $\omega = \sigma^2 = 1$)					
$\hat{\mu}_Z$	Mean	4.0039	3.9979	4.0007	4.0191
	SD	0.0124	0.0183	0.0328	0.0533
	CV	0.0031	0.0046	0.0082	0.0133
$\hat{\sigma}_Z$	Mean	0.9998	0.9978	1.0027	1.0076
	SD	0.0204	0.0220	0.0326	0.0643
	CV	0.0204	0.0220	0.0325	0.0638
$\hat{\gamma}_Z$	Mean	0.5042	0.5004	0.5018	0.5078
	SD	0.0339	0.0366	0.0487	0.0992
	CV	0.0673	0.0732	0.0970	0.1953
$\hat{\omega}$	Mean	1.0005	0.9970	1.0027	1.0153
	SD	0.0210	0.0228	0.0332	0.0691
	CV	0.0210	0.0229	0.0331	0.0680
$\hat{a}$	Mean	NA	2.0101	3.0412	5.9864
	SD	NA	0.0437	0.0708	0.2672
	CV	NA	0.0218	0.0233	0.0446
Size of simulation 40 × 40 ($\mu = 4$, $\gamma = 0.5$, $\omega = \sigma^2 = 1$)					
$\hat{\mu}_Z$	Mean	4.0001	3.9978	4.0075	4.0026
	SD	0.0244	0.0475	0.0573	0.1685
	CV	0.0061	0.0119	0.0143	0.0421
$\hat{\sigma}_Z$	Mean	1.0095	1.0030	1.0032	1.0149
	SD	0.0387	0.0522	0.0741	0.1156
	CV	0.0383	0.0520	0.0738	0.1139
$\hat{\gamma}_Z$	Mean	0.5058	0.4858	0.5029	0.4916
	SD	0.0615	0.0806	0.1065	0.1727
	CV	0.1215	0.1659	0.2118	0.3512
$\hat{\omega}$	Mean	1.0094	1.0029	1.0059	1.0340
	SD	0.0395	0.0516	0.0748	0.1173
	CV	0.0392	0.0515	0.0744	0.1134
$\hat{a}$	Mean	NA	2.0063	2.9974	6.2019
	SD	NA	0.0710	0.2810	0.6037
	CV	NA	0.0354	0.0937	0.0973

CV coefficient of variation

It's worthy to note that in implementing the above procedures a common covariance matrix Σ_Z or Σ_W can be used at nodes with the same geometric layout of the target node and its conditioning nodes. As illustrated in Fig. 4, nodes with the same geometric layout (marked by the same symbols) are associated with a common covariance matrix Σ_W. Utilizing this property helps to reduce the execution time for random field simulation. Such observation and property have been previously noted and applied by Bellin and Rubin (1996) in developing a HYDRO_GEN Gaussian random field simulation model.

5 Simulation and validation

As mentioned earlier, a stationary and isotropic random field $\{Z(x), x \in \Omega\}$ is completely characterized by its probability density $f_Z(x)$ and covariance function $C_Z(h)$ [or

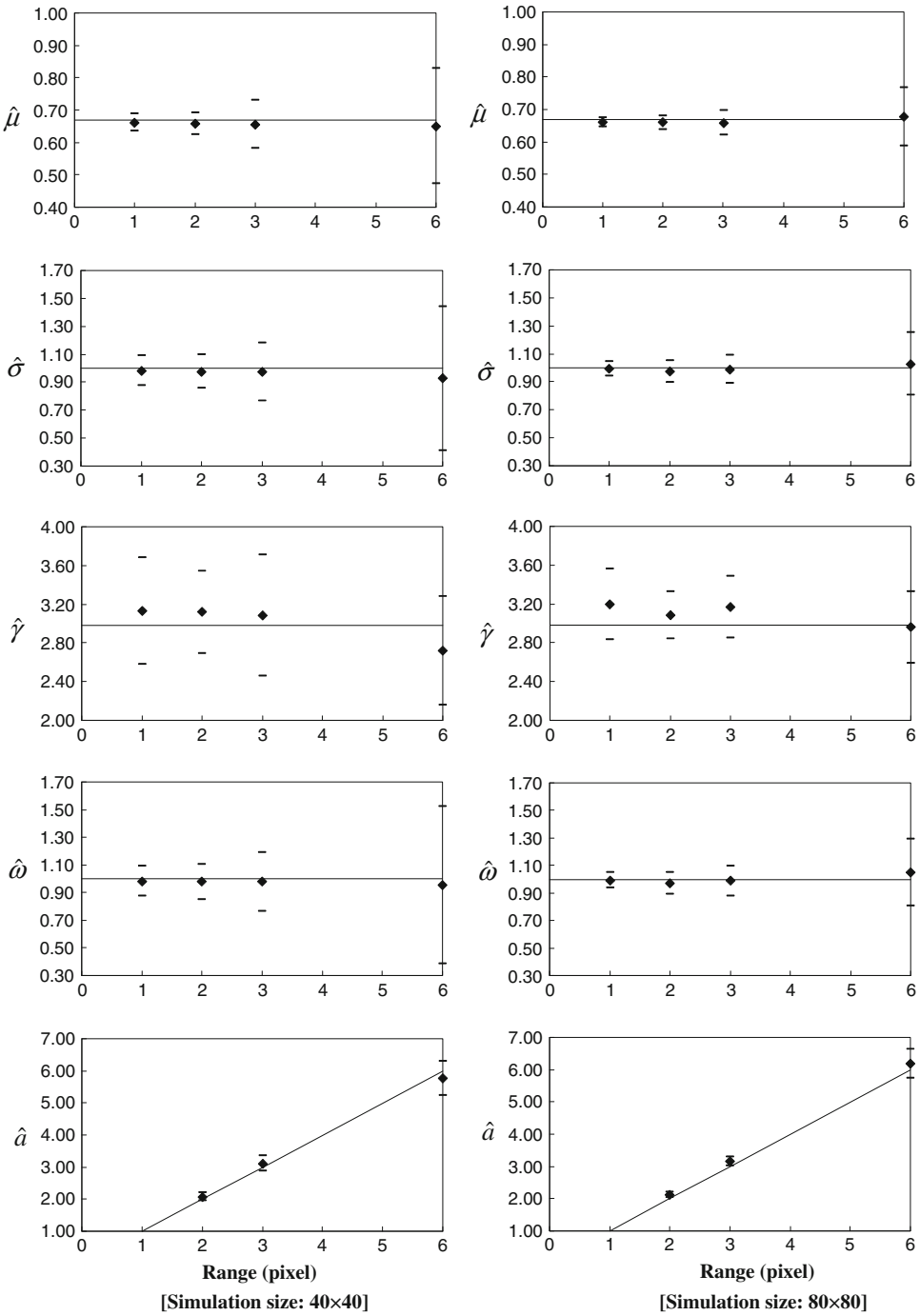

Fig. 5 Estimates of parameters of the density function and semi-variogram model (Scenario I). *Filled triangle* mean of the 100 sample estimates; *dash* one standard deviation from the sample mean. The *solid lines* represent the true parameter values

semi-variogram $\gamma_Z(h)$]. In order to demonstrate the implementation and validation of the proposed gamma random field simulation approach, four types of simulation scenarios using the spherical semi-variogram model were adopted for generation of realizations. As listed in Table 3, these simulation scenarios cover a range of coefficient of skewness from 0.5 to near 3.0. Range of the spherical semi-variogram model varies from 1 to 6 with respect to simulation sizes of 40 × 40 and 80 × 80. For the convenience of subsequent descriptions and display of the simulated data, the term "pixel" will be used to represent individual data points and the unit of distance between data points as well. Since our simulation is based on a discrete network of one pixel grid interval, the random field with one-pixel range is technically completely random with no spatial correlation between any neighboring pixels, resulting in a pure nugget semi-variogram. As the range increases, the degree of spatial correlation also increases. One hundred simulation runs were conducted for each scenario type with respect to specific values of range and simulation size.

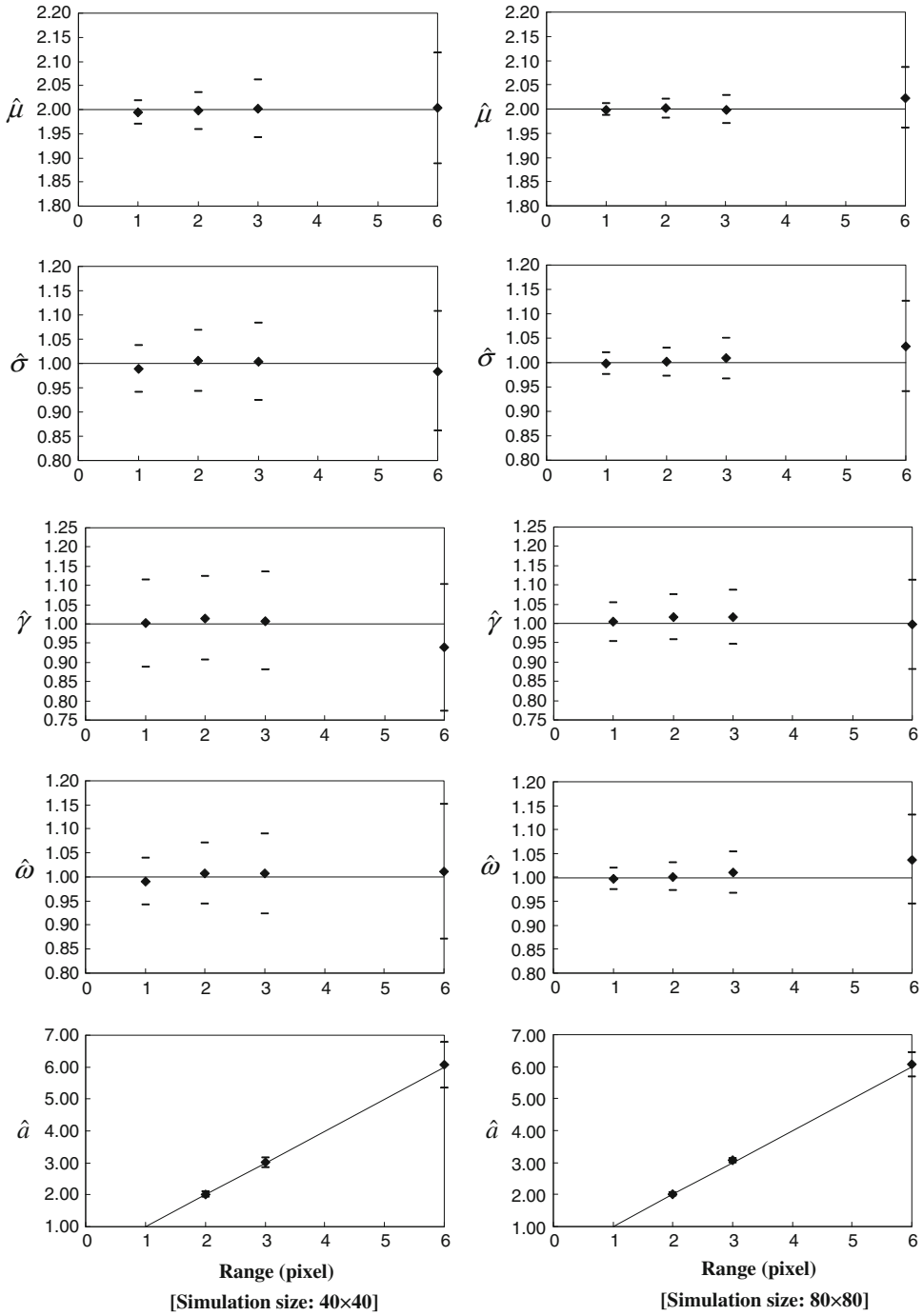

Fig. 6 Estimates of parameters of the density function and semi-variogram model (Scenario III). *Filled triangle* mean of the 100 sample estimates; *dash* one standard deviation from the sample mean. The *solid lines* represent the true parameter values

From each simulated realization, parameters of the gamma density were estimated using the following equations:

$$\hat{\mu}_Z = \frac{1}{N_\Omega}\sum_{x\in\Omega} z(x) \tag{23}$$

$$\hat{\sigma}_Z = \sqrt{\frac{\sum_{x\in\Omega}[z(x)-\hat{\mu}_Z]^2}{N_\Omega - 1}} \tag{24}$$

$$\hat{\gamma}_Z = \frac{N_\Omega}{(N_\Omega-1)(N_\Omega-2)\hat{\sigma}_Z^3}\sum_{x\in\Omega}[z(x)-\hat{\mu}_Z]^3 \tag{25}$$

where $\hat{\mu}_Z$, $\hat{\sigma}_Z$ and $\hat{\gamma}_Z$ are respectively estimates of the mean, standard deviation and coefficient of skewness of the random field, and N_Ω is the number of pixels in the simulation domain Ω, i.e. $N_\Omega = 6{,}400$ (80×80) or $1{,}600$ (40×40).

Parameters (sill ω and range a) of the spherical semi-variogram model were also estimated by the ordinary least squares fitting method. The method of ordinary least squares assumes that different data pairs involved in semi-variogram fitting are uncorrelated. Except for realizations with very short range as compared to the size of simulation, such assumption is a clear violation of the simulated realizations which are associated with certain spatial covariance matrix. Thus, it inevitably introduces higher degree of uncertainty in the process of parameter estimation. Other semi-variogram fitting methods such as the weighted least squares (Cressie 1985; Gotway 1991; Pardo-Iguzqúiza 1999) and the generalized least squares (Pardo-Iguzqúiza and Dowd 2001) have also been proposed, and the uncertainty of semi-variogram parameter estimation using these methods has also been addressed (Pardo-Iguzqúiza and Dowd 2001).

For a given scenario type and a specific value of range, parameter estimation was done for each of the 100 realizations. These estimates vary among different realizations. Therefore, the sample mean and standard deviation of these realization-specific parameter estimates $(\hat{\mu}_Z, \hat{\sigma}_Z, \hat{\gamma}_Z, \hat{\omega}, \hat{a})$ were calculated and tabulated in Tables 4, 5, 6, 7. Generally speaking, the estimated values are in very good agreement with the true parameter values, and the estimation uncertainty (characterized by the standard deviation

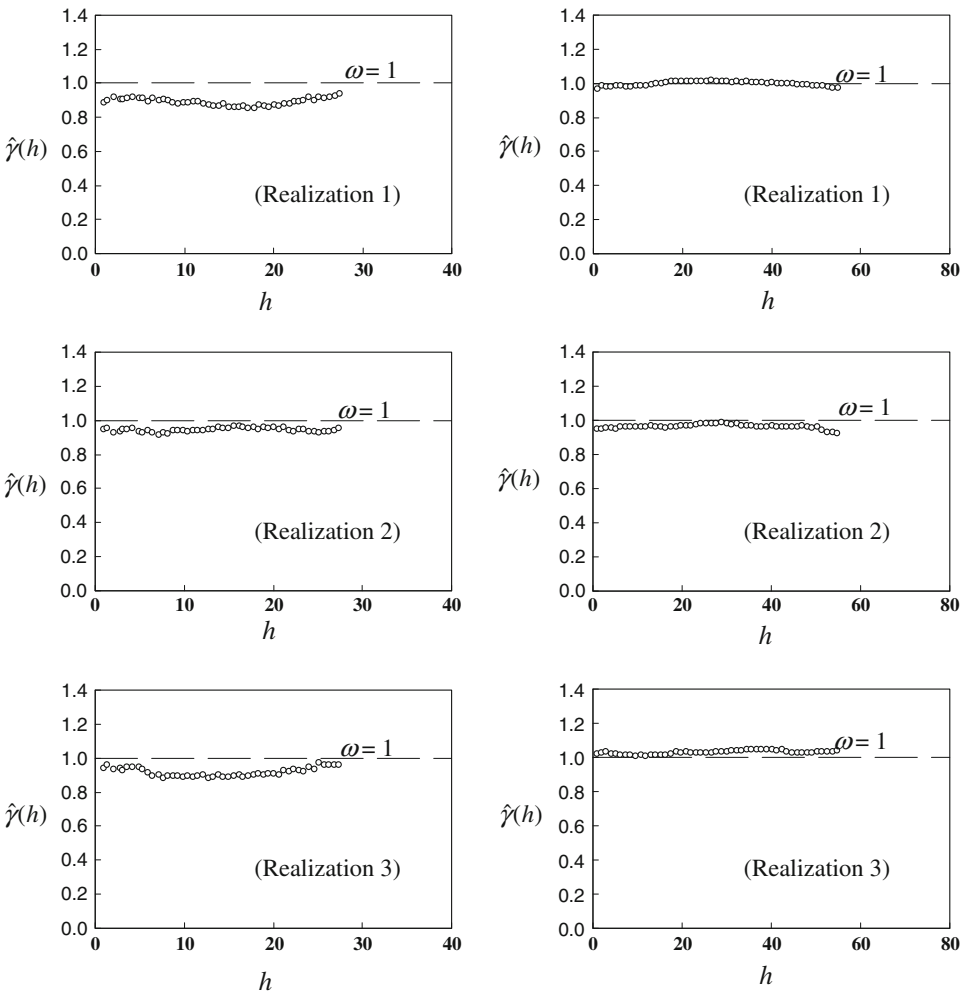

Fig. 7 Exemplar experimental semi-variograms $\hat{\gamma}(h)$of a pure random gamma field (Scenario I, $\mu = 0.67$, $\gamma = 2.985$, $\omega = 1$, $a = 1$). The experimental semi-variograms are seen to resemble a pure nugget semi-variogram

or coefficient of variation of the sample estimates) reduces with increasing simulation size N_Ω. Figures 5 and 6 also demonstrate that the estimation uncertainty introduced by assuming independence between data points increases with increasing spatial dependency (greater ranges) of the random field. It is worthy to note that since a random field with one-pixel range is technically pure random, no attempt was made to fit the spherical semi-variogram model to the corresponding experimental semi-variograms. A few examples of such experimental semi-variograms are shown in Fig. 7. All of them can be perfectly modeled as pure nugget semi-variograms, suggesting the simulated realizations are originated from the assigned pure random field. As the simulation size increases, sills of the experimental semi-variograms become closer to their theoretical value of $\omega = 1$.

To better demonstrate the capability of the proposed algorithm for generating random fields with desired properties, we randomly selected three simulated realizations of Scenario III (gamma density parameters: $\mu = 2$, $\gamma = 1$, $\alpha = 4$, $\lambda = 2$; variogram parameters: $\omega = 1$, $a = 3$) with simulation size $N_\Omega = 40 \times 40$, and compared the ECDFs and experimental semi-variograms against their theoretical counter parts. Figure 8 shows that the experimental variograms estimated by the ordinary least squares fitting method are very close the theoretical variogram with minor variation of sills due to sampling uncertainty, whereas the ECDFs coincide almost perfectly with the theoretical CDF. Finally, images of several simulated realizations of Scenario III are shown in Fig. 9. As the range a increases, higher degrees of spatial correlation become visually apparent.

It is worthy to note that in many real-world applications the covariance functions and ECDFs of the natural/environmental processes under investigation were derived from observed (or experimental) data, and that raises the question about situations in which the proposed approach can be applied. However, we argue that there are also situations

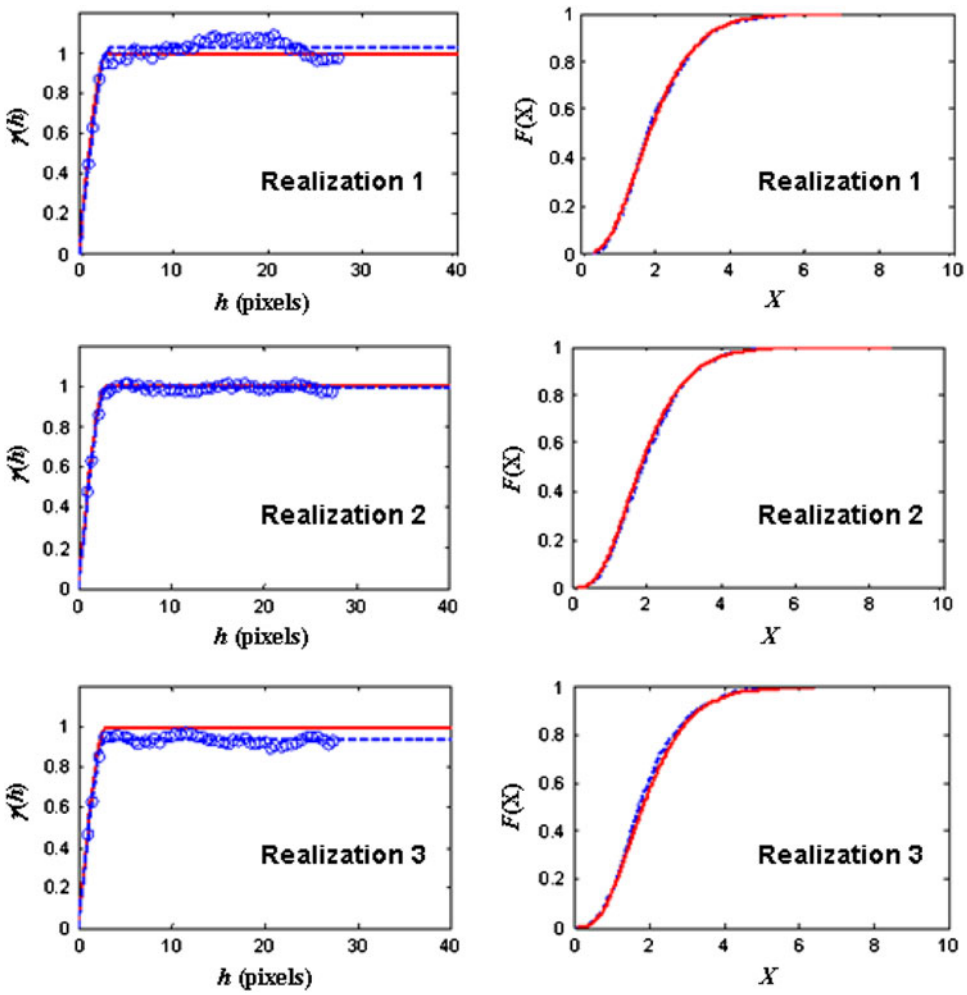

Fig. 8 Illustrative comparison of theoretical and estimated semi-variograms and CDFs for three simulated realizations of gamma random field of Scenario III ($\mu = 2$, $\gamma = 1$, $\alpha = 4$, $\lambda = 2$, $\omega = 1$, $a = 1$) with simulation size $N_\Omega = 40 \times 40$. *Solid lines* theoretical semi-variogram or CDF; *dotted lines* estimated semi-variogram or CDF

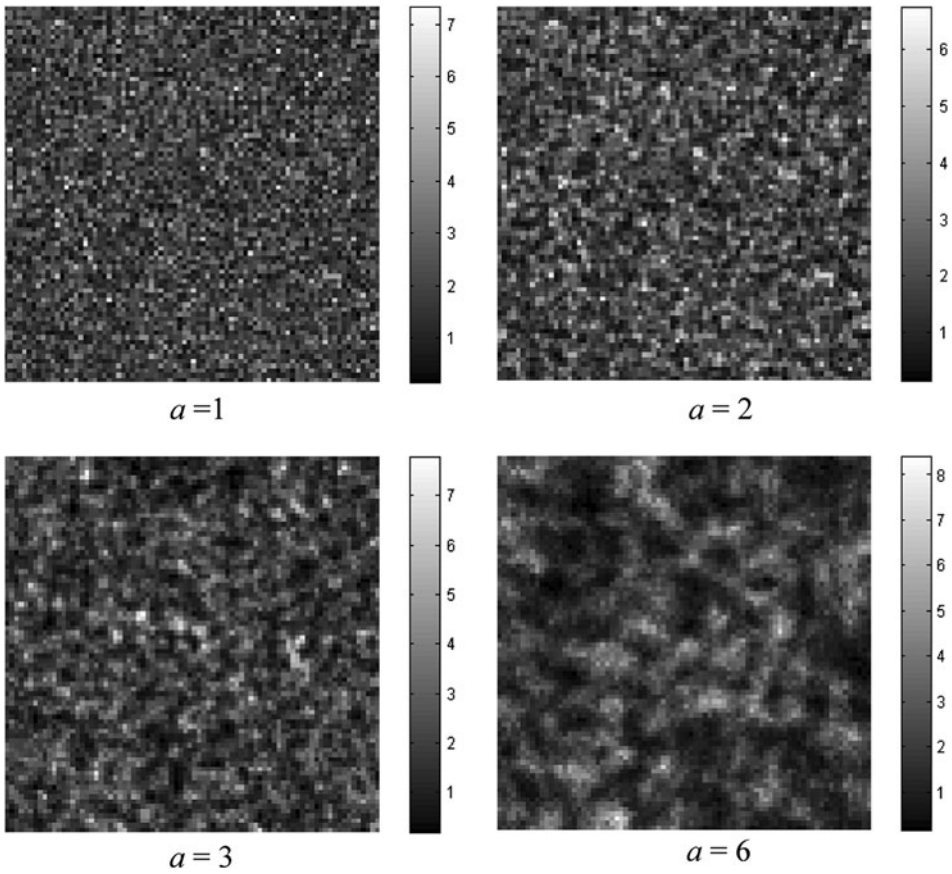

Fig. 9 Images of simulated realizations of a gamma random field (Scenario III, $\mu = 2$, $\gamma = 1$, size of simulation 80×80). *Grey* levels represent simulated values of the random field

in which experimental data are not available and we wish to make decisions based on *scenario-based* simulation results. For examples, evaluation of the potential impact of increasing land application rates on risks of heavy metal contamination in soils and the effect of climate change on high intensity and low frequency rainfalls, if the spatial rainfall variation is modeled as a gamma random field. In such scenario-based situations, we do not have experimental data, instead we assume values of model parameters and conduct simulations under such parameter scenarios. Setting model parameters for different scenarios is a crucial step in scenario-based simulation, and it should be based on our knowledge about the random processes of interest. Such knowledge may be drawn form historical data or scientific reasoning. In particular, the parameters should be set within a range which is physically feasible.

As a final note we emphasize that the proposed covariance matrix transformation approach can be generally applied for simulation of random fields of other distribution types (for example, the extreme-value type I distribution). Cheng et al. (2007) demonstrates that many distributions commonly used in hydrological frequency analysis can be simulated through a frequency-factor-based approach. Frequency factors of these distributions involve only the standard normal deviate. As a result, their bivariate distributions can be easily converted to corresponding bivariate standard normal distributions. Once the conversional relationship between correlation coefficients of the target bivariate distribution and bivariate normal distributions is established, the covariance matrix transformation approach proposed in this study can be implemented for simulation of the target random fields.

6 Conclusions

In this study we present a technique for gamma random field simulation. Such a technique can be applied to stochastic simulation of many natural phenomena which are asymmetric and can be characterized by a gamma random field. The proposed gamma random field simulation technique is composed of three sequential components: (1) covariance function conversion between a gamma random field and a corresponding Gaussian random field, (2) generating realizations of a Gaussian random field with standard normal density and the desired covariance function, and (3) transforming Gaussian realizations to

corresponding gamma realizations. Through a set of devised simulation scenarios, the proposed technique is shown to be capable of generating realizations of given gamma random fields. The approximation function of the gamma-Gaussian covariance conversion works well for coefficient of skewness of the gamma density not exceeding 3.0. Execution time for random field simulation using the proposed technique can be significantly reduced if the geometric pattern of the target pixel and its neighboring pixels are taken into consideration. The proposed gamma random field simulation technique may be very useful for risk assessment and spatial modeling of non-negative and asymmetric environmental variables.

Acknowledgements This research was originally initiated from a project funded by the Council of Agriculture, Taiwan, ROC. We thank two synonymous reviewers for providing constructive comments which were very helpful in addressing key issues.

Appendix 1: Proof of one-to-one mapping between x and w in Eq. 16

From the Wilson–Hilferty approximation and assuming the approximation to be exact, we have

$$x = \frac{\alpha}{\lambda}\left\{1 - \frac{1}{9\alpha} + w\sqrt{\frac{1}{9\alpha}}\right\}^3. \tag{26}$$

Differentiating x with respect to w yields

$$\begin{aligned}\frac{dx}{dw} &= \frac{\alpha}{\lambda}3\left\{1 - \frac{1}{9\alpha} + w\sqrt{\frac{1}{9\alpha}}\right\}^2\sqrt{\frac{1}{9\alpha}} \\ &= \frac{\sqrt{\alpha}}{\lambda}\left\{1 - \frac{1}{9\alpha} + w\sqrt{\frac{1}{9\alpha}}\right\}^2 \geq 0\end{aligned} \tag{27}$$

Let $\frac{dx}{dw} = 0$, we have

$$w = \frac{1 - 9\alpha}{3\sqrt{\alpha}} \tag{28}$$

Taking the second derivative of x with respect to w, it yields

$$\frac{d^2x}{dw^2} = \frac{\sqrt{\alpha}}{\lambda}2\left\{1 - \frac{1}{9\alpha} + w\sqrt{\frac{1}{9\alpha}}\right\}\sqrt{\frac{1}{9\alpha}} \tag{29}$$

Substituting (28) into (29),

$$\frac{d^2x}{dw^2} = 0 \quad \text{at} \quad w = \frac{1 - 9\alpha}{3\sqrt{\alpha}} \tag{30}$$

From Eqs. 27 and 30, we conclude that Eq. 26 is a one-to-one mapping function with an inflection point at $w = \frac{1-9\alpha}{3\sqrt{\alpha}}$.

Appendix 2: Proof of Eq. 17 as a unique conversion

Assuming the approximation of Eq. 17 to be exact and taking derivative of $\mathrm{COV}(X_1, X_2)$ with respect to $\rho_{W_1W_2}$, it yields

$$\frac{d}{d\rho_{W_1W_2}}\mathrm{COV}(X_1, X_2) = \frac{162}{6561\alpha_1^{0.5}\alpha_2^{0.5}\lambda_1\lambda_2}\left(\rho_{W_1W_2} - E\right)^2 \geq 0 \tag{31}$$

where

$$E = -\frac{162\alpha_1\alpha_2 - 18\alpha_1 - 18\alpha_2 + 2 - F^{0.5}}{18\alpha_1^{0.5}\alpha_2^{0.5}},$$

and

$$\begin{aligned}F = {} & 13122\alpha_1^2\alpha_2^2 - 4374\alpha_1^2\alpha_2 - 4347\alpha_1\alpha_2^2 + 1134\alpha_1\alpha_2 \\ & + 162\alpha_1^2 - 54\alpha_1 + 162\alpha_2^2 - 54\alpha_2 + 2.\end{aligned}$$

The covariance of two gamma random variable X_1 and X_2 monotonically increases with correlation coefficient of two corresponding standard normal random variables W_1 and W_2. Thus, Eq. 17 represents a unique conversion function.

References

Bellin A, Rubin Y (1996) HYDRO_GEN: A spatially distributed random field generator for correlated properties. Stoch Hydrol Hydraul 10:253–278

Best NG, Ickstadt K, Wolpert RL (2000) Spatial Poisson regression for health and exposure data measured at disparate resolutions. J Am Stat Assoc 95:1076–1088

Botter G, Porporato A, Rodriguez-Iturbe I, Rinaldo A (2007) Basin-scale soil moisture dynamics and the probabilistic characterization of carrier hydrologic flows: slow, leaching-prone components of the hydrologic response. Water Resour Res 43:W02417. doi: 10.1029/2006WR005043

Cheng KS, Wei C, Cheng YB, Yeh HC (2003) Effect of spatial variation characteristics on contouring of design storm depth. Hydrol Process 17:1755–1769

Cheng KS, Chiang JL, Hsu CW (2007) Simulation of probability distributions commonly used in hydrologic frequency analysis. Hydrol Process 21:51–60

Cheng KS, Hou JC, Liou JJ, Wu YC, Chiang JL (2010) Stochastic simulation of bivariate gamma distribution—a frequency-factor based approach. Stoch Environ Res Risk Assess. doi:10.1007/s00477-010-0427-7

Cressie N (1985) Fitting variogram models by weighted least squares. Math Geol 17(5):563–586

Deutsch CV, Journel AG (1992) GSLIB: Geostatistical Software Library and User's Guide. Oxford University Press, New York

Emery X (2008) Substitution random fields with Gaussian and gamma distributions: theory and application to a pollution data set. Math Geosci 40:83–99

Franco C, Soares A, Delgado J (2006) Geostatistical modelling of heavy metal contamination in the topsoil of Guadiamar river margins (S Spain) using a stochastic simulation technique. Geoderma 136:852–864

Goovaerts P (1997) Geostatistics for natural resources evaluation. Oxford University Press, New York

Gotway CA (1991) Fitting semi-variogram models by weighted least squares. Comput Geosci 17(1):171–172

Guillot G (1999) Approximation of Sahelian rainfall fields with meta-Gaussian random functions. Part 1: model definition and methodology. Stoch Environ Res Risk Assess 13:100–112

Herrick MG, Benson DA, Meerschaert MM, McCall KR (2002) Hydraulic conductivity, velocity, and the order of the fractional dispersion derivative in a highly heterogeneous system. Water Resour Res 38(11):1227–1239

Høst G, Berg E, Schweder T, Tjelmeland S (2002) A Gamma/Dirichlet model for estimating uncertainty in age-specific abundance of Norwegian spring-spawning herring. J Mar Sci 59:737–748

Journel A (1974) Geostatistics for conditional simulation of ore bodies. Econ Geol 69:673–687

Journel AG, Huijbregts CJ (1978) Mining geostatistics. Academic Press, London

Kan R (2008) From moments of sum to moments of products. J Multivar Anal 99:542–554

Kendall MG, Stuart A (1977) The advanced theory of statistics, vol 1: distribution theory, 4th edn. Charles Griffin, London

Minasny B, Hopmans JW, Harter T, Eching SO, Tuli A, Denton MA (2004) Neural networks prediction of soil hydraulic functions for alluvial soils using multistep outflow data. Soil Sci Soc Am J 68:417–429

Morrison DF (1990) Multivariate statistical methods, 3rd edn. McGraw-Hill, New York

Nieto-Barajas LE (2008) A Markov gamma random field for modelling disease mapping data. Stat Model 8(1):97–114

Niu GY, Yang ZL, Dickinson RE, Gulden LE (2005) A simple TOPMODEL-based runoff parameterization (SIMTOP) for use in global climate models. J Geophys Res 110(D21106). doi: 10.1029/2005JD006111

Pardo-Iguzqúiza E (1999) VARFIT: a Fortran-77 program for fitting variogram models by weighted least squares. Comput Geosci 25(3):251–261

Pardo-Iguzqúiza E, Dowd PA (2001) VARIOG2D: a computer program for estimating the semi-variogram and its uncertainty. Comput Geosci 27:549–561

Patel JK, Read CB (1996) Handbook of the normal distribution. Marcel Dekker, New York

Potter NJ, Zhang L, Milly PCD, McMahon TA, Jakeman AJ (2005) Effects of rainfall seasonality and soil moisture capacity on mean annual water balance for Australian catchments. Water Resour Res 41(W06007): doi:10.1029/2004WR003697

Rauch AF (1997) EPOLLS: An empirical method for predicting surface displacements due to liquefaction-induced lateral spreading in earthquakes. PhD dissertation, Virginia Polytechnic Institute and State University, Blacksburg, VA

Rodriguez-Iturbe I, Porporato A, Ridolfi L, Isham V, Cox D (1999) Probabilistic modelling of water balance at a point: the role of climate soil and vegetation. Proc R Soc Lond Ser A 455: 3789–3805

Vogler ET, Chrysikopoulos CV (2001) Dissolution of nonaqueous phase liquid pools in anisotropic aquifers. Stoch Environ Res Risk Assess 15:33–46

Wolpert RL, Ickstadt K (1998) Poisson/gamma random field models for spatial statistics. Biometrika 85:251–267

Zeng N, Shuttleworthc JW, Gash JHC (2000) Influence of temporal variability of rainfall on interception loss—part I. Point analysis. J Hydrol 228:228–241